Indian J. Met. Hydrol. Geophys. (1975), **26**, 3, 326-332

551.509.332 (54)

An experiment in forecasting with diabatic baroclinic model over India and neighbourhood

T. K. MUKERJI and R. K. DATTA

Northern Hemisphere Analysis Centre, New Delhi

ABSTRACT. This paper contains the results of experiments in forecasting the flow patterns over India and neighbourhood at 850, 700, 500 and 300-mb levels with the help of a four-layer quasi-geostrophic diabatic model. The effects of the ground contour, latent heat of condensation and radiation have been taken into account for computation of the vertical velocity ω. To bring out the salient features of the model in this paper, we present the results of a case study.

1. Introduction

The Northern Hemisphere Analysis Centre at New Delhi, India, prepares on a regular basis, prognostic charts valid for the next 24 hr, using conventional methods. Computerised prognostic charts are also being prepared there regularly. This was originally being prepared with a non-divergent barotropic model (Datta *et al.* 1969) and was later changed to a divergent barotropic model (Mukerji and Datta 1971). Although the results obtained from the barotropic models are fairly useful, there are obvious limits to their performance. Apart from theoretical limitations, the main practical difficulties are, firstly it does not show developments of weather systems, and secondly, the forecast is confined to only 500-mb level. Since both these drawbacks are inherent in any barotropic model it was decided to develop a multilayer baroclinic model.

The first multilayer model to be tried for forecasting was an adiabatic 4-layer model (Mukerji and Datta 1972). Apart from neglecting the diabatic effects, other simplifications which were incorporated into this model were :

(*i*) Effect of ground contour was not taken into account,

(*ii*) The vertical velocity at 1000 and 200 mb level were assumed to be zero, and

(*iii*) Effect of radiation was considered to be negligible. The input data and forecast for this model were contour heights of 900, 700, 500 and 300-mb levels. The ω values were computed at 800, 600 and 400-mb levels every hour.

The present model is an improvement of the adiabatic model, wherein, all the effects neglected previously, have been incorporated. This is necessary, since most of the time the model is required to undertake prognosis of fields which include cyclonic storms over sea as well as disturbances over hilly terrain, and clearly the simplified model developed earlier is incapable of handling the same.

2. The basic equations

The equations of baroclinic flow can be written as,

$$\frac{\partial \zeta}{\partial t} + V_g . \nabla \eta = f_0 \frac{\partial \omega}{\partial p} \qquad (2.1)$$

where,

$$\zeta = \frac{g}{f} . \nabla^2 z, \eta = \zeta + f \text{ and } V_g = -\frac{g}{f} \nabla z \times \mathbf{k} \qquad (2.1a)$$

$$\text{and } \frac{\partial}{\partial t}\left(-\frac{\partial \phi}{\partial p}\right) + V . \nabla\left(-\frac{\partial \phi}{\partial p}\right) - S\omega = \frac{R}{c_p P} \frac{dQ}{dt} \qquad (2.2)$$

where, $S = -\alpha \frac{\partial \ln \theta}{\partial p}$

and dQ/dt is the non-adiabatic rate of heating per unit time per unit mass.

A list of the symbols is given in Appendix I.

From these two equations is derived the quasi-geostrophic ω equation by eliminating the time dependent term, using geostrophic relation. This is given by

$$\nabla^2 \omega + \frac{f_0^2}{S} \frac{\partial^2 \omega}{\partial p^2} = \frac{1}{S}\left[\frac{\partial}{\partial p} J(\phi, \eta) + \frac{1}{f_0} \nabla^2 \left\{ J\left(\phi, -\frac{\partial \phi}{\partial p}\right)\right\} - \frac{R}{c_p P} \nabla^2 \frac{dQ}{dt}\right] \qquad (2.3)$$

This eqation being lin ear in ω can be solved in two part which are

$$\nabla^2\omega_1+\frac{f_0^2}{S}\frac{\partial^2\omega_1}{\partial p^2}=\frac{1}{S}\left[\frac{\partial}{\partial p}J\left(\phi,\ \eta\right)+\frac{1}{f_0}\nabla^2\left\{J\left(\phi,-\frac{\partial\phi}{\partial p}\right)\right\}\right] \quad (2.4)$$

$$\nabla^2\omega_2+\frac{f_0^2}{S}\frac{\partial^2\omega_2}{\partial p^2}=-\frac{1}{S}\frac{R}{c_pP}\nabla^2\frac{dQ}{dt} \quad (2.5)$$

The final value of vertical velocity is given by

$$\omega=\omega_1+\omega_2 \quad (2.6)$$

Once ω is obtained, it is substituted into Eq. (2.1) and the tendencies of contours at grid points are obtained. A time step of 1 hr is used to obtain the forecast values of the contours. The whole process is repeated 24 times to arrive at the final forecast for 24 hr.

3. Inclusion of the effect of latent heat of condensation

dQ/dt in the equations of the previous section is produced by latent heat of condensation, sensible heat, radiation etc. Thus we can write $dQ/dt = dQ_L/dt + dQ_S/dt + dQ_R/dt$. Eq. (2.5) being linear, it can be split up for each of the contributing terms above and solved separately for vertical velocity. In this section we will discuss first two terms and the effect of radiation is discussed separately in Section 4. The vertical velocity is now given by $\omega_2=\omega_L+\omega_S$ and $\omega=\omega_1+\omega_L+\omega_S$.

The parameterisation of dQ_L/dt has been made as suggested by Gambo (1963). Thus

$$dQ_L/dt=-LdV_{SAT}/dt=-\omega\,L\,F^* \quad (3.1)$$

F^* is the condensation rate and is a function of T and x only. In Eq. (3.1) ω appears explicitly, which is yet to be computed. As such ω, which is obtained by solution of Eq. (2.4) is used as a first approximation for ω. Alternately since ω_S can be computed independently $\omega'=\omega_1+\omega_S$ can be used as a first approximation for ω and in the present study this procedure has been followed. Thus the equation for obtaining ω_L is given by

$$\nabla^2\omega_L+\frac{f_0^2}{S}\frac{\partial^2\omega_L}{\partial p^2}=-\frac{1}{S}\frac{R}{c_pP}\nabla^2(-\omega'\,L\,F^*) \quad (3.2)$$

Saito (1969) has given approximate values of the term LRF^*/c_pP for different pressure levels and different ranges of temperatures. These have been utilised in solution of Eq. (3.2) and are reproduced in Appendix II. It will be seen from these expressions that, values of LRF^*/c_pP can only be computed if the temperatures T at the grid points, at different pressure levels are available. For this study T values at 400, 600 and 200-mb levels have been computed from the geopotential values at 300, 500, 700 and 900-mb levels by hydrostatic relationship. Thus every hour a new set of values of T is computed.

4. Inclusion of radiation effect

The heat that is produced due to release of latent heat of condensation keeps on adding to the system. After the process of prognostication has advanced by a few hours, the total heat builds up to such an extent as to vitiate the whole solution. It is assumed that this heat gets radiated out and is distributed equally in the area of integration. Thus, following a simple method of compensating for radiation effect is adopted. The total average of heat generated at all the grid points is computed and the average of the same is subtracted from every grid point after integration for each hour. This will in turn modify the vertical velocity.

5. Inclusion of sensible heat

Parameterisation of sensible heat was done as per Spar (1962). Thus,

$$\frac{dQ_S}{dt}=A|V|(T_S-T_a)\left(\frac{P}{P^*}\right)^\gamma \quad (5.1)$$

dQ_S/dt gives the rate of heating per unit time and unit mass, at the pressure level P. P^* is surface pressure and T_S and T_a are temperatures of the surface water and surface air. The constants are $A=1.0\times10^{-4}$ m/sec/deg and $\gamma=2$ (Manabe 1958). V gives the surface wind speed.

Since T_S, T_a and V are all unknown over the sea area, some arbitrary values are to be used in computations. Alternately, help may be taken of the few ship reports which are available from the Bay of Bengal and Arabian Sea areas. Since the latter process is indefinite, average values were used for the calculations. However, it was observed that with the average values, the effect on vertical velocity ω due to sensible heat exchanges is very little. As such, in the final analysis, the effect of sensible heat was left out.

6. Construction of the grid

Horizontal grid — The horizontal grid has a grid length of 381 km in both x- and y- directions true at Lat. 22½°N. The numbers of grid points are 31 in the abscissa and 16 in the ordinate, making a total of 496. The area of computation and the area for which the final forecast is valid, are shown in Fig. 1. A mercator projection chart is used with a scale of $1:20\times10^6$ true at Lat. 22½°N.

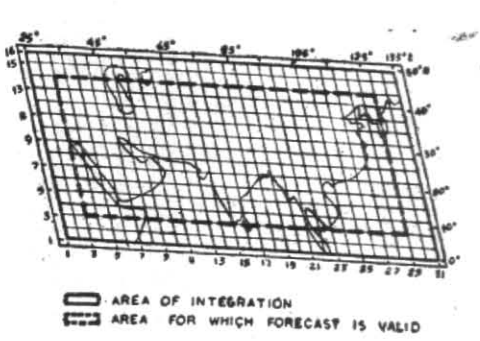

Fig. 1. Horizontal grid

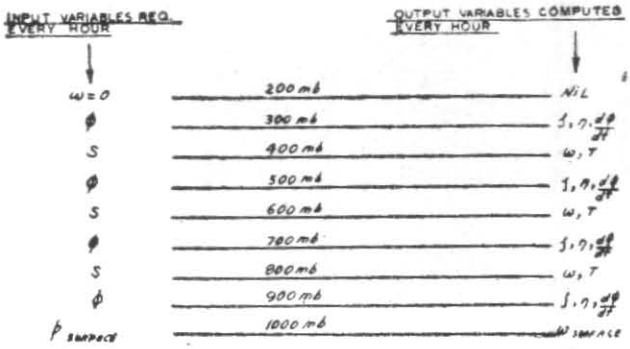

Fig. 2. Vertical grid—Input and output variables

Vertical grid — In the vertical, the area of computation is bounded by the ground surface at the bottom and the 200-mb level at the top. The different layers for which input data of contour heights are fed are 300, 500, 700 and 900 mb. The value of the grid distance in the vertical thus becomes 200 mb. The input values of parameters required and the forecast values of the same, together with other details of the vertical grid are shown in Fig. 2.

7. Boundary conditions, other constraints and constants

In order to solve the equations mentioned in Sections 2 and 3 by numerical relaxation methods, it is necessary to prescribe certain boundary conditions. For this study these boundary condition are as follows:

Vertical velocity ω at 1000 mb — This is computed from the geopotential values and 900 mb and the grid point values of ground contour. The method used is given by the equation

$$\omega_{1000} = V_{1000} \cdot \nabla P_{\text{surface}}$$

As a first approximation the wind velocity at 1000 mb, V_{1000} has been taken to be the same as at 900 mb and computed from the contour values at the grid points with the help of geostrophic relationship. The standard pressure at the surface (P_{surface}) is computed from the grid point ground contour values.

The values of ω at 200 mb level — This is taken as zero. Considering the fact that in the tropics the tropopause is near 200-mb level, this assumption is not likely to produce large inaccuracies. However, other methods for computation of ω_{200} are available (Lateef 1968) and will be utilised in future modifications.

Lateral boundary values — The values of tendencies of contour, at the lateral boundaries are taken to be zero. This was arrived at after testing with different boundary conditions, like allowing the boundary values to float by giving the neighbouring values etc. In the latter cases no significant impovement in forecast could be seen. Since the area of interest lies away from the boundaries, this boundary condition is not likely to have adverse effects on the short period (24 hr) forecast itself.

Ellipticity condition — Some criteria has to be satisfied, so that ellipticity condition of Eq. (3.2) is maintained. This is necessary for the solution of the ω equation to converge. The criteria used is that $LRF^*/c_pP - S < 0$. Whenever this criteria is not satisfied, LRF^*/c_pP is artificially made equal to $0.8 \times S$.

Static stability values — Average static stability parameter values for each level have been interpolated from published data (Mukerji *et al.* 1972). Thus for each of the levels, 400, 600 and 800 mb, a single value of S is known. These values of S have to be changed each month.

Coriolis parameter — The coriolis parameter has been taken as a constant, keeping in mind the conservation of K.E. and vorticity. f_0 has been given the value of coriolis parameter for latitude 22½°N. However for computation of η the absolute vorticity f has been treated as a variable.

Input data — Since the input data comprises grid point contour values, they are directly obtained from the charts of 300, 500 and 700-mb levels. The contour values of 900-mb level are obtained from those of 850-mb level by uniformly subtracting 500 gpm from all grid point values. Although this is a very approximate method, it seems to give acceptable results.

8. Case study

The forecasts obtained by the application of the above model to the data of 28 October 1972

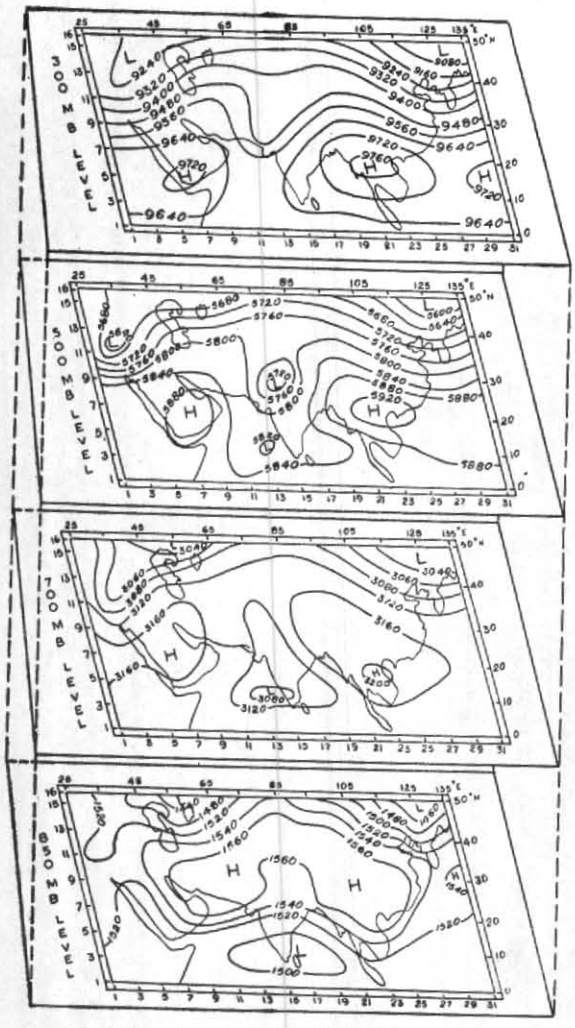

Fig. 3. Input contours (gpm) of 28 October 1972 at 00 GMT

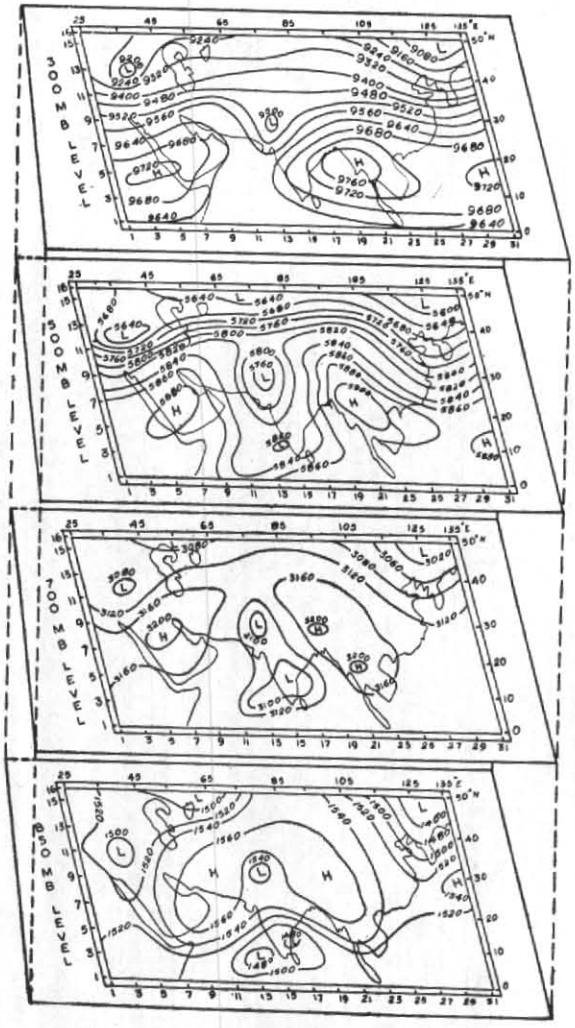

Fig. 4. Predicted contours (gpm) valid 29 October 1972 at 00 GMT

are presented here. The input charts of 28 October, the forecast charts and the realised charts on 29 October are shown in Figs. 3, 4 and 5 respectively.

Initial synoptic situation — At 850-mb level of the input charts (Fig. 3) an extended low pressure area lay over the southern Peninsula of India and adjoining sea area. A trough line extended from central parts of India towards northnorthwest upto Lat. 31.7°N. A deep trough was located near the western boundary, extending from Lat. 24.8°N, Long. 32.4°E to Lat. 45.9°E, Long. 39.8°N. Another well marked trough was situated roughly in between the Caspian Sea and the Aral Sea.

The 700 mb chart shows a low pressure area with centre near Lat. 11.1°N and Long. 69.4°E. In addition to this a trough of low is seen extending from central parts of India towards northnorthwest. A trough near the western boundary along Lat. 34.8°N is similar to the one described for the 850-mb level. The high pressure areas are well marked and are situated over Arabia and Indo-China.

At 500-mb level, there is well marked low pressure area (commonly known in India as western disturbance) with centre near Lat. 28.5°N, Long. 73.1°E, with a trough extending into the Arabian Sea. Another trough of low lies over Arabian Sea. A low pressure area lies with centre near Lat. 37.7°N and Long. 32.4°E.

At the 300-mb level, a deep trough of low exists roughly along Long. 39.4°E. Another deep trough exists westnorthwest of Caspian Sea. Two high pressure cells are located over Arabia and Burma with one more cell to the extreme east.

Comparison with forecast chart — The forecast charts (Fig. 4) for all the levels can now be compared with the input charts (Fig. 3) to find the movement and intensificatin or weakening of the systems. They can also be compared with the actual charts of 29 October 1972 (Fig. 5) to check the accuracy of the forecasts.

At 850 mb level cut-off low pressure areas have been produced where only troughs existed before. The centres of these are at Lat. 31.5°N, Long. 76.8°E and Lat. 35°N, Long. 36.1°E. A comparison with the realised charts show that both these low pressure areas have really formed although their centres differ by about 3° longitude in the former and 1° longitude in the latter. Keeping in mind the fact that the centres shown in the realised chart may themselves be in error due to paucity of data, the forecasts seem to be reasonably correct. Two other new low pressure areas are shown in the forecast over the southern Peninsula, where only a trough of low existed before. These are also borne out to be correct by the realised chart. The deep trough lying between Caspian Sea and Aral Sea has become feeble and moved to the east by about 7.5° longitude.

Taking the 700 mb forecast, it is seen that the low pressure are a over Arabian Sea has become a trough of low, whereas in the realised chart it is still, shown as a low pressure area. Since the low, on the realised chart is not based on any data, but put there from considerations of continuity only, the forecast does not appear to be in much error. A feeble low pressure area has formed over extreme northwest India and agrees with the realised position. Another feeble low pressure area has been generated with central position near Lat. 37.7°N and Long. 36.1°E and agrees well with the actual on 29 October 1972. The central region of the high pressure area over Indo-China has moved westwards by about 4° of longitude. The other high over Arabia also has moved westward at its northern periphery. These agree well with the realised situation.

At the 500 mb level, the well marked western disturbance of the input chart has been weakened in the forecast chart by about 40 gpm but has not moved. However the trough extending southwards has moved east by about a grid length. Comparison with the realised situation shows that its speed has been predicted to be slower than actual. The other low pressure area in the Arabian Sea seems to have moved away across the boundary. A fresh low has developed in the Arabian Sea, but is not seen in the realised chart. The low pressure area near Lat. 37·7°N and Long. 312·4°E has moved in the forecast chart by on

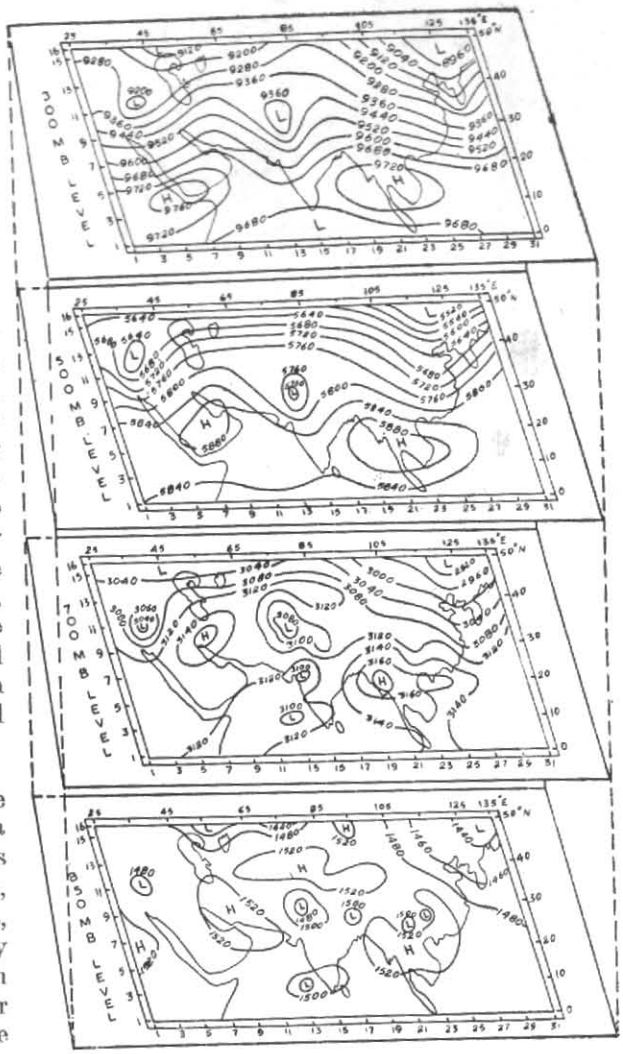

Fig. 5. Actual contour (gpm) of 29 October 1972 at 00 GMT

grid length and agrees fairly well with the realised charts. The central regions of high pressure areas over Indo-China and Arabia have also shown considerable westward movement.

300 mb forecast chart also shows good agreement with the realised chart of 29 October 1972. The centres of low pressure areas near Lat. 28·6°N, Long. 73·3°E and Lat. 46·6°N, Long. 36·1°E are in agreement with the actual. The direction of movement of the high pressure cells over Burma and Arabia also seem to be in the right direction.

Further comments on forecast evaluation — In the above comparisons between the forecast charts valid for 29 October 1972 and the realised charts of the same day, stress has been placed on the major systems, their generation, dissipation and movement. However, a further comparison

is necessary between the orientation and delineation of the contour lines themselves. In a number of cases it is found that the delineations in the forecast are different from those on the realised charts. Also, in some cases, like the western disturbance over northwest India at 300 mb, proper amount of intensification has not been produced in the forecast. In addition, systems which are of wavelength smaller than about 1000 km have got lost in the forecast. These seem to be some of the drawbacks of the forecast model in its present form.

It is also noticed that the results of application of adiabatic version of the present model to the above data do not differ much from the results obtained with this diabatic model. This may be attributed to the meagre release of latent heat as very little rainfall occurred in association with the system studied.

9. Concluding remarks

Although a number of case studies have been made with the model discussed in this paper, for economy only one has been presented here. Other cases involved cyclonic storms and low pressure areas moving inland across the east coast of India from the Bay of Bengal. From these experiments the following tentative results can be arrived at :

(*i*) This model is capable of forecasting movement of large scale synoptic systems over the Indian area with fair degree of accuracy.

(*ii*) Generation of new low pressure areas over regions, where only trough existed earlier, is done correctly. Dissipation of weather systems is also prognosticated properly.

(*iii*) Delineation and values of contour lines in the forecasts differ from the realised ones, in many cases.

(*iv*) Weather systems smaller than 1000 km in wavelength are smoothed out in the forecasts.

It is desired to modify this model in the light of experience gained, after case studies for various synoptic situations are completed. Statistical tests, of verification can then be applied to compute the root mean square error in the forecast.

It is also proposed to apply rigorous scheme incorporating radiation effect and convective adjustments especially for the forecasts of validity of 48 and 72 hours.

Acknowledgements

The authors are indebted to Shri D. Krishna Rao, Director, Northern Hemisphere Analysis Centre, New Delhi, India for making this study possible and to Dr. P. Koteswaram, Director General of Observatories, India Meteorological Department for granting permission to communicate these results. We are also gratefull to Shri Harikishan for preparation of the diagrams and to Shri J. K Wahi for typing the manuscript.

REFERENCES

Datta, R.K., Chhabra, B.M. and Singh, B.V.	1969	India met. Dep. Sci. Rep. No. 112, pp. 1-7.
Gambo, K.	1963	*J. met. Soc. Japan*, Ser. II, **41**, pp. 233-246.
Lateef, M. A.	1967	*Mon. Weath. Rev.*, **25**, pp. 781-782.
Manabe, S.	1958	*J. met. Soc. Japan*, Ser. II, **36**, pp. 123-133.
Mukerji, T. K. and Datta, R. K.	1972	India met. Dep. Sci. Rep. No. 189, pp. 1-11.
Mukerji, T. K., Shaikh, Z. E. and Gupta, R .N.	1972	*Indian J. Met. Geophys.*, **23**, 1, pp. 57-66.
Saito, N.	1960	*Tech. Rep.*, No. 3, Japan Met. Agency.
Spar, J.	1962	A vertically integrated wet, diabatic model for the study of cyclogenesis. Proc. Int. Symp. on NWP in Tokyo, pp. 185-204.